

HaploBlocker: Creation of Subgroup-Specific Haplotype Blocks and Libraries

Torsten Pook,^{*,†,1} Martin Schlather,^{†,*} Gustavo de los Campos,[§] Manfred Mayer,^{**} Chris Carolin Schoen,^{**} and Henner Simianer^{*,†}

^{*}Department of Animal Sciences, Animal Breeding and Genetics Group, University of Goettingen, 37075, Germany, [†]Center for Integrated Breeding Research, University of Goettingen, 37075, Germany, [‡]Stochastics and Its Applications Group, University of Mannheim, 68159, Germany, [§]Departments of Epidemiology and Biostatistics and Statistics and Probability, Institute for Quantitative Health Science and Engineering, Michigan State University, Michigan 48824, and ^{**}Plant Breeding, Technical University of Munich School of Life Sciences Weihenstephan, 85354 Freising, Germany

ORCID IDs: 0000-0001-7874-8500 (T.P.); 0000-0001-5692-7129 (G.d.l.C.); 0000-0003-2687-8316 (M.M.)

ABSTRACT The concept of haplotype blocks has been shown to be useful in genetics. Fields of application range from the detection of regions under positive selection to statistical methods that make use of dimension reduction. We propose a novel approach ("HaploBlocker") for defining and inferring haplotype blocks that focuses on linkage instead of the commonly used population-wide measures of linkage disequilibrium. We define a haplotype block as a sequence of genetic markers that has a predefined minimum frequency in the population, and only haplotypes with a similar sequence of markers are considered to carry that block, effectively screening a dataset for group-wise identity-by-descent. From these haplotype blocks, we construct a haplotype library that represents a large proportion of genetic variability with a limited number of blocks. Our method is implemented in the associated R-package HaploBlocker, and provides flexibility not only to optimize the structure of the obtained haplotype library for subsequent analyses, but also to handle datasets of different marker density and genetic diversity. By using haplotype blocks instead of single nucleotide polymorphisms (SNPs), local epistatic interactions can be naturally modeled, and the reduced number of parameters enables a wide variety of new methods for further genomic analyses such as genomic prediction and the detection of selection signatures. We illustrate our methodology with a dataset comprising 501 doubled haploid lines in a European maize landrace genotyped at 501,124 SNPs. With the suggested approach, we identified 2991 haplotype blocks with an average length of 2685 SNPs that together represent 94% of the dataset.

KEYWORDS haplotype blocks; haplotype libraries; population genetics; selection signatures; R-package; identity-by-descent

OVER the years, the concept of haplotype blocks has been shown to be highly useful in the analysis of genomes. Applications can be found in a variety of fields, including fine-mapping in association studies (Druet and Georges 2010; Islam *et al.* 2016), genomic prediction (Meuwissen *et al.* 2014; Jiang *et al.* 2018), and mapping of positive selection

in specific regions of the genome (Sabeti *et al.* 2002, 2007). Haplotype blocks can also be used as a dimension reduction technique (Pattaro *et al.* 2008; Fan *et al.* 2014) that produces features that are potentially more informative than individual single nucleotide polymorphisms (SNPs) (Zhang *et al.* 2002; Wall and Pritchard 2003).

Existing methods commonly define a haplotype block as a set of adjacent loci, using either a fixed number of markers or a fixed number of different sequences of alleles per block (Meuwissen *et al.* 2014). Alternatively, population-wide linkage disequilibrium (LD) measures (Daly *et al.* 2001; Gabriel *et al.* 2002; Taliun *et al.* 2014; Kim *et al.* 2017) can be used in the identification process to provide more flexibility of block size based on local genetic diversity. The methods and software [e.g., HaploView, (Barrett *et al.* 2005)] available for

Copyright © 2019 by the Genetics Society of America

doi: <https://doi.org/10.1534/genetics.119.302283>

Manuscript received May 6, 2019; accepted for publication May 30, 2019; published Early Online May 31, 2019.

Available freely online through the author-supported open access option.

Supplemental material available at FigShare: <https://doi.org/10.25386/genetics.7862525>.

¹Corresponding author: University of Goettingen, Department of Animal Sciences, Center for Integrated Breeding Research, Animal Breeding and Genetics Group, Albrecht-Thaer-Weg 3, 37075 Goettingen, Germany. E-mail: torsten.pook@uni-goettingen.de

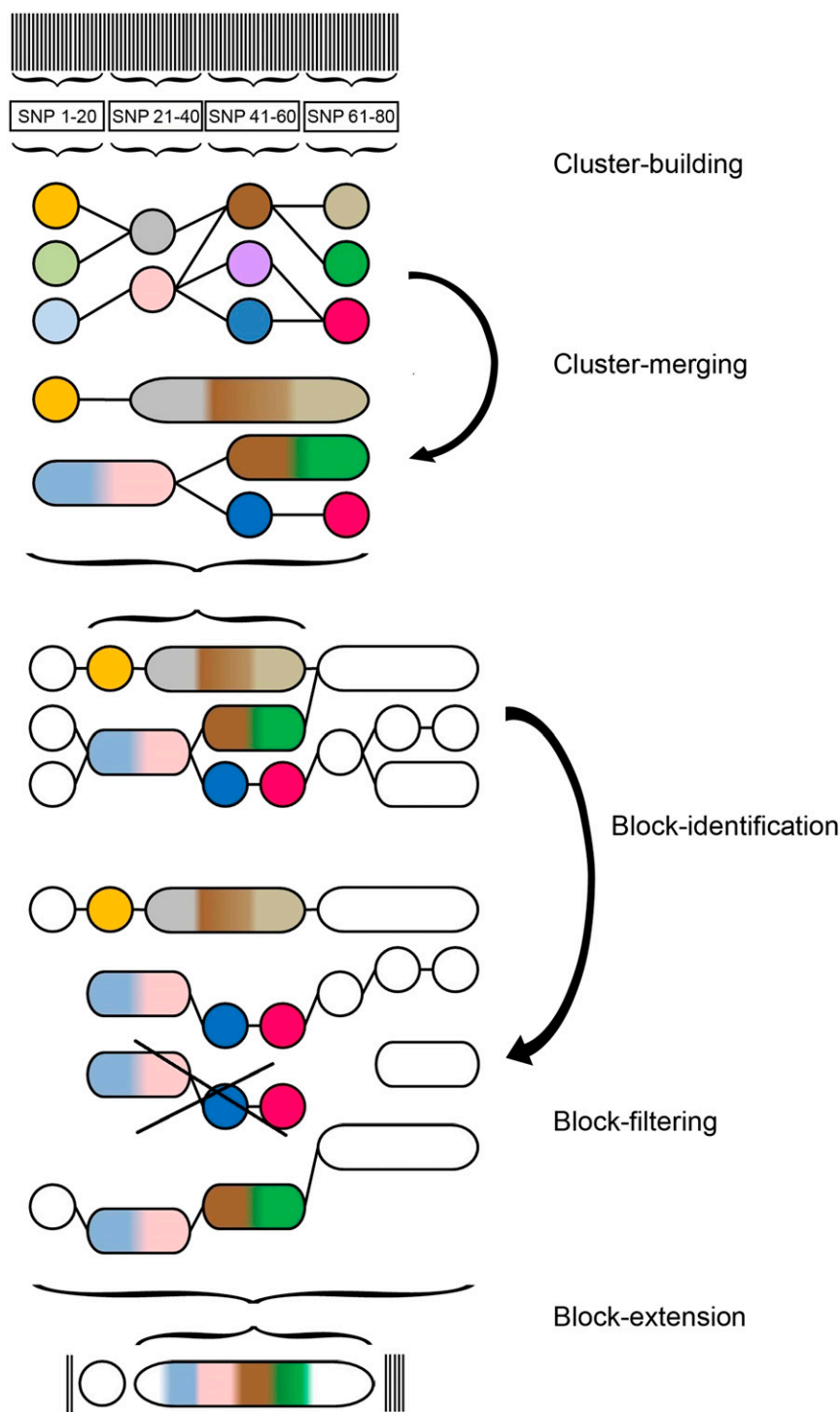


Figure 1 Schematic overview of the steps of the HaploBlocker method: (1) Cluster-building: classifying local allelic sequences in short windows into groups. (2) Cluster-merging: simplifying window cluster by merging and neglecting nodes. (3) Block-identification: identifying blocks based on transition probabilities between nodes. (4) Block-filtering: creating a haplotype library by reducing the set of blocks to the most relevant ones for the later application. (5) Block-extension: extending blocks by single windows and SNPs. The same allelic sequences in different steps are coded with the same colors in the graph.

inferring haplotype blocks have become increasingly sophisticated and efficient. Although those approaches to infer haplotype blocks have been proven useful, existing methods share some key limitations (Slatkin 2008). In particular, the use of population-wide measures of LD limits the ability of existing methods to capture cases of high linkage characterized by the presence of long shared segments caused by absence of crossing over (typically within families or close ancestry). To illustrate this, consider the following toy

example of four different haplotypes: 11111111, 10101010, 01010101, and 00000000. If all four haplotypes have the same frequency in the population, the pairwise LD (r^2) of adjacent SNPs is zero and LD-based algorithms would not retrieve any structure. However, in this example, knowledge of the first two alleles fully determines the sequence in the segment.

In this work, we use the term “allele” for a genetic variant. This can be a SNP or other variable sites like short indels. We

Table 1 Exemplary dataset of allelic sequences and their assignment according to the cluster-building-step

Frequency	Allelic sequence	Group
101	00011	1
54	11111	3
40	11110	3
3	10011	1
2	01001	2

use the term “haplotype” for the sequence of alleles of a gamete. This always refers to the full gamete, and, explicitly, not a local and short sequence of alleles. Lastly, a combination of multiple adjacent alleles is here referred to as an “allelic sequence.”

As the starting point of our approach (“HaploBlocker”), we assume a set of known haplotypes that can be either statistically determined as accurately phased genotypes, or observed via single gamete genotyping from fully inbred lines or doubled haploids. When the interest is in inferring the longest possible shared segment between haplotypes, a common approach is to identify segments of identity-by-descent (IBD). A tool for the identification of IBD segments is BEAGLE (Browning and Browning 2013), among others. Since IBD is typically calculated between pairs of individuals, a screening step is used to identify haplotypes that are shared by multiple individuals, *e.g.*, by the tool IBD-Groupon (He 2013). A method to detect IBD segments directly for groups of individuals has been proposed by Moltke *et al.* (2011), but is not applicable to datasets with hundreds of haplotypes due to limitations of computing times. A further difficulty is that common methods are not robust against minor variation, leading to actual IBD segments being broken up by calling errors [0.2% with the later used Affymetrix Axiom Maize Genotyping Array (Unterseer *et al.* 2014)] and other sources of defects.

The imputation algorithm of BEAGLE uses a haplotype library given by a haplotype cluster (Browning and Browning 2007). The haplotype library in BEAGLE, which is used to initialize a Hidden Markov Model for the imputing step, is only given in a probabilistic way. This means that there are no directly underlying haplotype blocks that could be used for later statistical application.

Our goal is to provide a conceptualization of haplotype blocks that can capture both population-wide LD and subgroup-specific linkage, and does not suffer from some of the limitations of IBD-based methods. Unlike common definitions that consider haplotype blocks as sets of adjacent markers, we define a haplotype block as an allelic sequence of arbitrary length.

Haplotypes with a similar sequence are locally assigned to the same block. Haplotype blocks are subgroup specific, so that a recombination hot spot appearing in a subgroup of haplotypes does not affect the boundaries of other blocks. This leads to very long blocks, which can cover the same region of

the genome, but may vary in the allelic sequence they represent. Even an overlap between the allelic sequences represented by different haplotype blocks is possible.

Subsequently, we start with a large set of identified haplotype blocks and reduce this set to the most relevant blocks and thus generate a condensed representation of the dataset at hand. We define this representation as a haplotype library, and, depending on the topic of interest, selection criteria for the relevance of each block can be varied appropriately to identify predominantly longer blocks or focus on segments shared between different subpopulations. The usage of haplotype blocks instead of SNPs allows the use of a variety of new methods for further genomic analyses since the number of parameters is usually massively reduced and haplotype blocks provide a natural model for local epistatic interactions.

Materials and Methods

The aim of HaploBlocker is to represent genetic variation in a set of haplotypes with a limited number of haplotype blocks as comprehensively as possible. The standard input of HaploBlocker is a phased SNP dataset. In the associated R-package HaploBlocker (R Core Team 2017; Pook and Schlather 2019) this input can be provided via the variant call format (VCF; Danecek *et al.* 2011), PLINK Flat files (PED/MAP; Purcell *et al.* 2007) or in a plain matrix object with each column containing a haplotype. For graphical reasons, haplotypes in all examples and figures in the manuscript are displayed in a row. The output of HaploBlocker is a haplotype library that can, in turn, be used to generate a block dataset. A block dataset contains dummy variables representing the presence/absence of a given block (0 or 1), or, in case of heterozygotes, a quantification of the number of times (0, 1, or 2) a block is present in an individual. The main idea of our method is to first consider short windows of a given length and increase the length of the analyzed segments in an iterative procedure involving the following steps:

- Cluster-building.
- Cluster-merging.
- Block-identification.
- Block-filtering.
- Block-extension.
- Target-coverage (optional).
- Extended-block-identification (optional).

Before we elaborate on each step in the following subsections, we give an outline of the three major steps. For a schematic overview of HaploBlocker, we refer to Figure 1. In the first step, we derive a graphical representation of the dataset (“window cluster”) in which a node represents an allelic sequence, and an edge indicates which, and how many, haplotypes transition from node to node (cluster-building). As locally similar allelic sequences are grouped together, this step also handles robustness against minor deviations (*e.g.*, calling errors). In the second major step, we identify candidates for the haplotype library based on the window cluster.

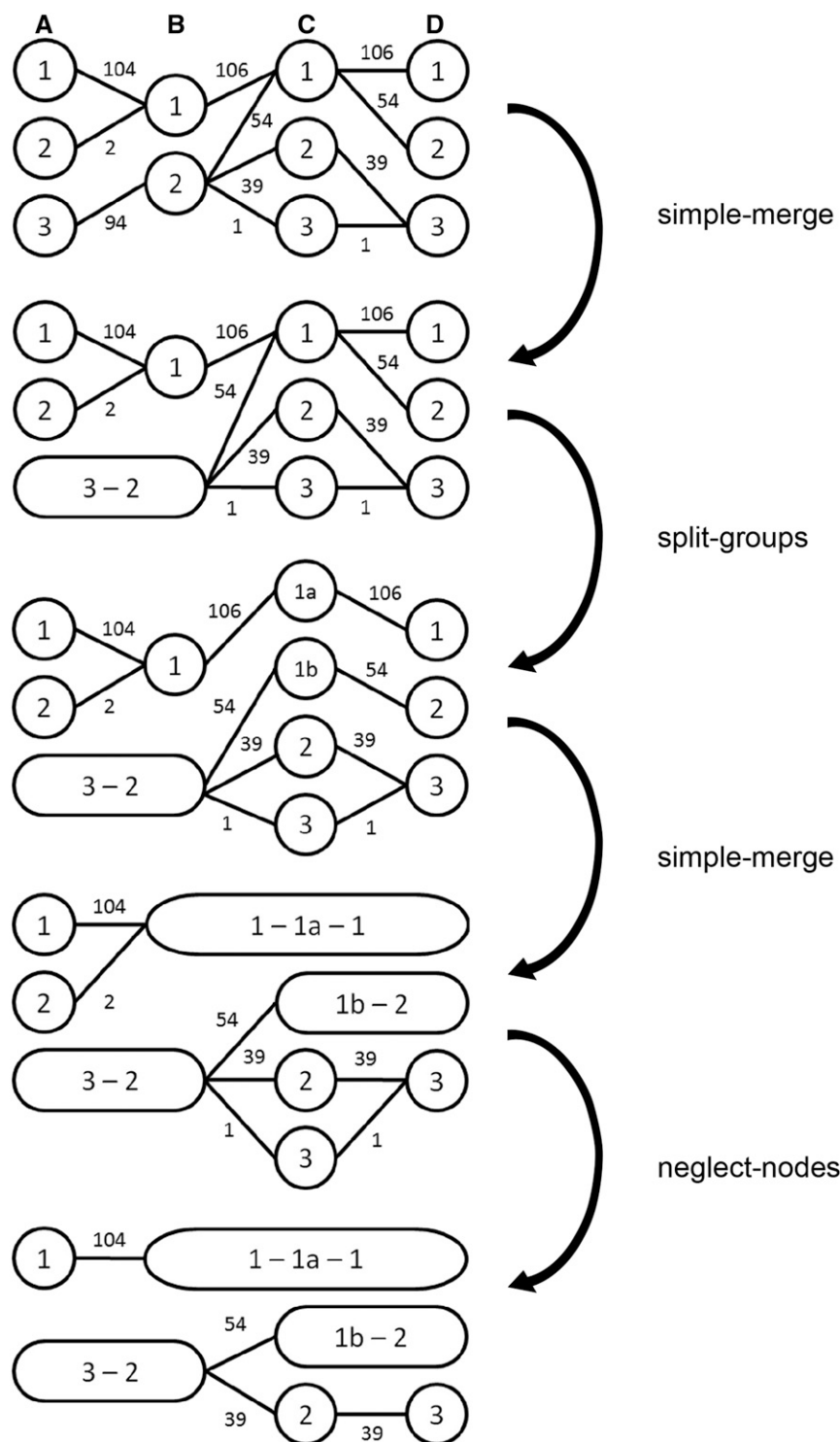


Figure 2 The four parts of the cluster-merging step. Haplotype frequencies in the window A are according to the toy example given in Table 1.

We call this step block-identification and use it to generate a large set of haplotype blocks. In the third and last major step (block-filtering), the set of candidates is reduced to the most relevant haplotype blocks, and, thereby, the haplotype library is generated. In addition to specifying the physical position of each block, we have to derive which haplotypes are included. The fact that blocks are subgroup specific makes the identification of the most relevant blocks complicated, so we split

this task into two separate, but closely connected steps (block-identification and block-filtering).

Minor steps in our procedure are cluster-merging and block-extension. The former reduces the computing time in the subsequent steps, whereas the latter increases the precision of the result. However, neither step has a major impact on the resulting haplotype library. Since various parameters are involved in the procedure, their value might be chosen by

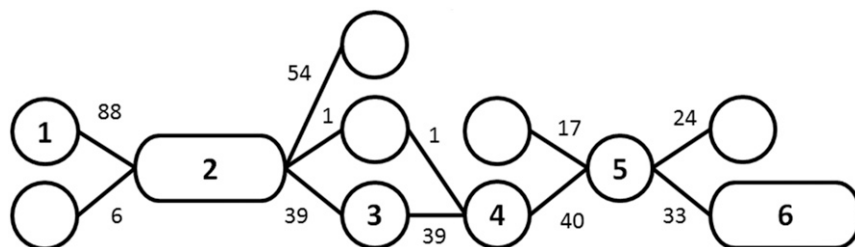


Figure 3 Excerpt of a window cluster. This included all edges (transitions) from the nodes of one of the common paths in the example dataset.

means of an optimization approach and/or a dataset can be processed with multiple parametrizations in the cluster-building, cluster-merging, and block-identification steps. For more details, we refer to the subsections on target-coverage (Supplemental Material, File S1) and extended-block-identification.

The next subsections deal with the graphical depiction of the haplotype library and the information loss incurring through the suggested condensation of genomic data. Subsequently, we discuss possible applications, namely the ability of our method to recover founder haplotypes of a population and a block-based version of extended haplotype homozygosity (EHH; Sabeti *et al.* 2002) and integrated extended haplotype homozygosity (IHH; Voight *et al.* 2006). In the last subsection, we introduce the datasets used in this study. Our method, as well as all discussed applications, are available for users by the correspondent R-package HaploBlocker (R Core Team 2017; Pook and Schlather 2019). The default settings of the arguments in the R-package correspond to the thread of the following subsections.

Cluster building

In the first step of HaploBlocker, we divide the genome into nonoverlapping small windows of size 20 markers as a default value. Accordingly, each haplotype is split into short allelic sequences. To account for minor deviations, we merge groups with similar allelic sequences as follows. For a fixed window, different allelic sequences are considered successively based on their frequency, starting with the most common one. In cases where less common allelic sequences differ only in a single marker, they are merged to a group. The allelic sequence of a group (“joint allelic sequence”) in each single marker is the most common allele of all contained haplotypes. Usually this will be the most frequent allelic sequence, but, when allowing for more than one deviation per window, this is not necessarily the case anymore. As a toy example, consider a group containing 4×11111 , 3×10110 , 2×00111 with a resulting joint allelic sequence of 10111. This robustness against errors may lead to actually different haplotypes to be grouped together. In later steps, we will introduce methods to split these haplotypes into different blocks if necessary. The choice of 20 markers as the window size, and a deviation of, at most, one marker as a default, is not crucial and should not have a major effect as long as the window size is much smaller than the later identified haplotype blocks. We will present ways to use flexible window sizes in the extended-block-identification step.

As an example, consider a SNP dataset with 200 haplotypes and five markers, given in Table 1. The two most common sequences form separate groups (00011 and 11111). For graphical reasons in later steps, we assign 11111 to group 3 even though it is the second group created. The next allelic sequence (11110) is assigned to the group of 11111, as it differs only in a single allele, and the joint allelic sequence remains 11111. In case an allelic sequence could join different groups, it is added to the group containing more haplotypes. Based on the groupings, we are able to create a graph, called a window cluster (Figure 2, top graph). Here, each node represents a group (and, thus, a joint allelic sequence), and the edges indicate how many of the haplotypes of each node transition into which adjacent node.

Cluster merging

A window cluster can be simplified without losing any relevant information for later steps of the algorithm. We apply three different techniques:

- simple-merge (SM): Combine two nodes if all haplotypes of the first node transition into the same adjacent node, and no other haplotypes are in the destination node.
- split-groups (SG): Split a node into two if haplotypes from different nodes transition into the same node and split into the same groups afterward.
- neglect-nodes (NN): Remove a node from the cluster if it contains a very small number of haplotypes—say, five. These removed haplotypes are still considered when calculating transition probabilities between nodes in later steps.

Since the only loss of information in this step stems from neglecting nodes, we first alternately apply SM and SG until no further changes occur. Next, we apply the sequence of NN, SM, SG, SM until fixation of the window cluster. We neglect rare nodes, since a block with few haplotypes (in the most extreme case a block with one haplotype over the whole genome) does not reflect much of the population structure, and would have little relevance for further genomic analyses. It should be noted that the minimum number of haplotypes per node in NN does not depend on the number of haplotypes in the sample. This is done mainly to ensure a similar structure of the later obtained haplotype library when adding haplotypes from a different subpopulation. Nevertheless, the option to modify this parameter is given, in case one is mostly interested in more common, or even rarer, allelic sequences.

Table 2 Influence of MCMB on the haplotype library for chromosome 1 in the KE DH-lines

MCMB	Number of Blocks	Average block length (# of SNPs)	Haplotypes per Block	Coverage (%)
1	1720	1117	159.9	97.2
1,000	878	1892	132.1	96.5
2,500	621	2345	120.3	95.6
5,000	477	2575	114.9	94.4
10,000	362	3022	103.9	92.7
20,000	274	3339	99.2	90.1
50,000	150	3894	98.5	81.2

As an example for the cluster-merging step, consider a dataset with four windows and five different sequences of groups (104× 1111, 54× 3212, 39× 3223, 2× 2111, 1× 3233, Figure 2). Haplotypes in the first window are chosen according to Table 1. In the first step, nodes A3 and B2 are merged by SM. Next, node C1 is split into two nodes via SG. This triggers additional SMs (B1-C1a-D1 and C1b-D2). Afterwards, SM or SG are no longer possible, and NN is performed, removing A2 and C3. No further SM or SG are possible after this. Consider that, even though D3 is the only node following C2, no SM is possible because removed haplotypes are still considered in later transition probabilities, and, therefore, D3 contains one more haplotype than C2.

Block identification

In the third step of HaploBlocker, we identify the haplotype blocks themselves. As a haplotype block in HaploBlocker is defined as a common allelic sequence in an arbitrarily large window, we use common sequences of nodes in the previously obtained window cluster as a first set of haplotype blocks. The identification process itself is performed by using each node as a starting block. The boundaries of each starting block are given by the boundaries of the node, and the allelic sequence is derived by its joint allelic sequence. A block is extended iteratively if $\geq 97.5\%$ of the haplotypes in a block transition into the same node; deviating haplotypes are removed. Haplotypes filtered out in this step can rejoin the block if their allelic sequence matches that of the joint allelic sequence of the final haplotype block in $\geq 99\%$ of the markers. The joint allelic sequence is derived by computing the most common allele in each marker for the contained haplotypes. The choices of 97.5 and 99% worked well in our tests, but any value close, but not equal, to 100% should work here. This again allows the user some flexibility in how long (in terms of physical length) the haplotype blocks should be, and how different jointly considered haplotypes are allowed to be. In a similar way, each edge of the window cluster is used as a starting block. Here, boundaries are given by the boundaries of the two connected nodes. The haplotype blocks identified here will not all be part of the final haplotype library but instead are just a set of candidates from which the most relevant ones will be selected in the block-filtering-step. Note that the share of allowed deviations in this step (1%) is lower

than in the cluster building (1 of 20 markers; 5%), since the size of the identified segment is longer than a single window, and the total number of deviations should get closer to the expected number (Unterseer *et al.* 2014).

To illustrate the method, consider the excerpt of a window cluster given in Figure 3. Nodes 2, 3, 4 represent the sequence of groups 3223 of Figure 2. When considering the second node as a starting block, we cannot extend the block because there are multiple possible nodes for the contained haplotypes [beforehand: nodes with 88 (93.6%) and 6 (6.4%); afterward: 54 (57.4%), 1 (1.1%), 39 (41.5%)]. When using the fourth node of the excerpt, the block can be extended until the second and fifth node of the cluster, since 39 of the 40 haplotypes transition (97.5%) into the same adjacent node. One ends up with the same block when using the third node or the edges, including 39, 39, and 40 haplotypes. In case all included haplotypes transition into the same node in the first window, the block could be extended even further. Note that, in this step, different allelic sequences of the same node (*cf.* cluster-building-step) can be in different haplotype blocks if they transition into different nodes in later steps [e.g., 11111 (54) and 11110 (39 + 1)] in the first window (Figure 2 and Table 2). For an extension to further increase the size of the set of haplotype blocks, we refer to the extended-block-identification step.

Block filtering

After the derivation of a set of candidates in the block identification, we reduce the set of all haplotype blocks to a haplotype library of the most relevant blocks to represent a high proportion of the dataset with a small number of blocks. First, we compute a rating r_b for each block b that depends on its length (l_b) and the number of haplotypes (n_b) in it:

$$r_b = l_b^{w_l} \cdot n_b^{w_n}.$$

Here, w_l and w_n represent weighting factors with default values $w_l = 1$ and $w_n = 1$. Note that only the ratio between both parameters matters.

Based on these ratings, we determine which haplotype block is the most relevant in each single cell/entry of the SNP dataset matrix. Iteratively, the blocks with the lowest number of cells as the most relevant block are removed from the set of candidates, until all remaining blocks are the most relevant block in a given number of cells. For this, we will later use the abbreviation MCMB (minimum number of cells as the most relevant block). For our datasets, 5000 was a suitable value for MCMB, but, without prior information, we recommend to set a target on what share of the SNP dataset is represented by at least one block (“coverage”). For details on the fitting procedure, we refer to File S1. In the case of the example given in Figure 3, we end up with block b_1 (green in Figure 4), including 94 haplotypes ranging from window 2 to 3 (node 2) with a rating $r_{b_1} = 940$ and block b_2 (red in Figure 4) ranging from window 2 to 6 (nodes 2,3,4,5) with a rating $r_{b_2} = 975$. To simplify the example, we assume that no other blocks have

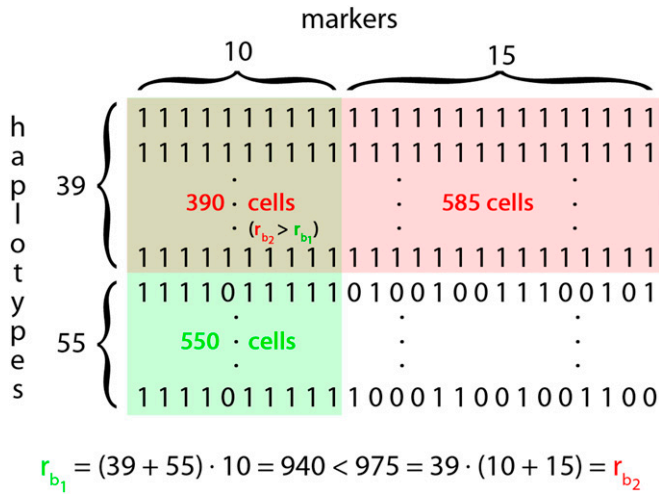


Figure 4 Toy example for the calculation in the block-filtering-step with $w_l = w_n = 1$.

been identified. b_2 has a higher rating; therefore, cells containing both blocks are counted as cells with b_2 as the most relevant block. This leads to b_1 having 550 cells of the SNP dataset as the most relevant block, and b_2 having 975.

It should be noted here that blocks in the final haplotype library can overlap. If MCMB is ≤ 550 , overlap occurs in our example, and typically can be observed when a short segment is shared in the majority of the population and a smaller subgroup shares a longer segment that includes the short segment. This will lead to dependencies in the presence/absence of blocks, which can be addressed in a similar way as LD between markers.

Even if w_l or w_n is set to zero, there is still an implicit weighting on both the length and the number of haplotypes since each haplotype block has to cover a certain number of cells of the SNP dataset (MCMB). The overall effect of w_l and w_n is higher when more candidates were created in the block-identification step.

Block extension

The haplotype blocks that have been identified in the previous step are limited to the boundaries of the nodes of the window cluster. Haplotypes in the blocks will transition into different adjacent nodes since the block was previously not extended (*cf.* block-identification). Nevertheless, different nodes can still have the same allelic sequence in some adjacent windows.

First, haplotype blocks are extended by full windows if all haplotypes are in the same group (*cf.* cluster-building) in the adjacent window. If the haplotypes of a specific block transition into different groups in the adjacent window, the block is still extended if there is no variation in the following 20 windows. By doing this, we account for possible errors that could have been caused by, for instance, translocations or phasing issues. The choice of 20 windows is again rather arbitrary, and should be chosen according to the minimum length of the blocks one is interested in. The chosen default results in a

Table 3 Influence of the window size on the haplotype library for chromosome 1 in the KE DH lines

Window size	Number of Blocks	Average block length (# of SNPs)	Haplotypes per Block	Coverage (%)
5	488	2489	121.8	93.5
10	482	2544	113.7	93.6
20	477	2575	114.9	94.4
50	474	2615	101.4	95.0

relatively large chunk of ≥ 400 SNPs (20 windows \times 20 markers) with all haplotypes of the block required to be classified in the same group for these windows (*cf.* cluster-building). These conservative settings are chosen because the adjacent segment can also be detected as a separate haplotype block. In any case, all SNPs with variation in a block are identified and reported in the outcome as a possible important information for later analyses.

Second, blocks are extended by single adjacent SNPs following similar rules as the window extension. As a default, we do not allow for any differences here, since haplotypes in the block must have some difference in the adjacent window. If working with a large number of haplotypes, and aiming to identify the exact end of a block, one might consider allowing for minor differences.

Extended block identification (optional)

When extending a haplotype block in the block-identification step, haplotypes transitioning into a different node are removed. Instead, one could consider both the short segment with all haplotypes and the long segment with fewer haplotypes. As the number of candidates is massively increased, it is recommended to consider the long segment only when at least a share t of haplotypes transition into that node. In our tests, $t = 0.95$ was a suitable value for this. Overall, this procedure will lead to the identification of even longer haplotype blocks as candidates for the haplotype library.

To obtain even more candidates in the block-identification step, one might compute multiple window clusters under different parameter settings (especially concerning window sizes). This provides additional robustness of the method. Especially in the case where the haplotype blocks finally obtained are short, the relevant haplotype blocks can be identified only with a low window size in the cluster-building step.

Both extensions require substantially more computing time, and, thus, are not included in the default settings of the associated R-package HaploBlocker (R Core Team 2017; Pook and Schlather 2019). The R-package contains an adaptive mode using window sizes of 5, 10, 20, or 50 markers, and a target coverage of 90%.

Graphical representation of haplotype blocks

We suggest a graphical representation of a haplotype library to display transition rates between blocks in analogy to

Table 4 Influence of the weighting of block length (w_l) and number of haplotypes (w_n) on the haplotype library for chromosome 1 in the KE DH lines

w_l	w_n	Number of Blocks	Average block length (# of SNPs)	Haplotypes per Block	Coverage (%)
1	0	470	2902	89.3	94.4
1	0.2	464	2900	94.1	94.4
1	0.5	463	2900	98.4	94.4
1	1	477	2575	114.9	94.4
0.5	1	532	2218	139.0	94.6
0.2	1	803	1518	189.5	95.5
0	1	1313	934	208.2	96.1

bifurcation plots (Sabeti *et al.* 2002; Gautier and Vitalis 2012). This requires ordering of the haplotypes according to their similarity in and around a given marker. For technical details on the sorting procedure, we refer to File S2.

Assessment of information content of haplotype blocks

HaploBlocker provides a condensed representation of the genomic data. We next discuss how to quantify the amount of information lost in the process of condensing a SNP dataset to a block dataset. At a recent conference, de los Campos (2017) proposed three methods for estimating the proportion of variance of an omics set (e.g., high-dimensional gene expression data, methylation or markers) that can be explained by regression on another type of omics data. We used a modified version of the second method proposed by de los Campos (2017) to estimate the proportion of variance of the full SNP dataset that can be explained by a regression on the blocks of a haplotype library. For computations in this work, the R-packages sommer (Covarrubias-Pazaran 2016; R Core Team 2017) and minqa (Powell 2009) were used, with overall very similar results. The methodology can be described briefly as follows:

In traditional SNP-based genomic models (Meuwissen *et al.* 2001), a phenotype (y) is regressed on a SNP dataset (X) using a linear model. Entries in X are usually 0, 1, or 2, with dimensionality being the number of individuals (n) times the number of markers (p).

$$y = Xb + \varepsilon,$$

assuming that the markers only have additive effects b . Hence, the vector of genomic values $g = Xb$ is a linear combination of the SNP genotypes. In order to estimate the proportion of g explained by the haplotype library, we regress the genomic values g onto the block dataset represented by a $n \times q$ matrix Z , say, of entries 0,1,2. Here q is the number of blocks, with q usually being much smaller than p :

$$g = Za + \delta.$$

From this perspective, genomic prediction based on haplotype blocks searches for a vector Za that is optimal in some sense.

Table 5 Influence of using the extended-block-identification on the haplotype library in dependency of the parameter t of the extended-block-identification-step for chromosome 1 in the KE DH lines

t	Number of Blocks	Average block length (# of SNPs)	Haplotypes per Block	Coverage (%)
1	477	2,575	114.9	94.4
0.95	603	5,659	89.8	94.6
0.9	788	9,371	70.2	95.2
0.8	916	11,716	60.9	95.5
0.6	970	12,430	58.5	95.7

For instance, in ridge regression, such a vector is obtained by minimizing a penalized residual sum of squares. It has to be noted that ε is an error term that includes nongenetic effects, whereas δ is an error term resulting from genetic effects that cannot be explained by additive effects (a) of single blocks. In random effect models, the proportion of the variance of g explained by linear regression on the haplotype library can be estimated using either Bayesian or likelihood methods like REML (Patterson and Thompson 1971). The proportion of variance explained will vary from trait to trait. We estimate the distribution of the proportion of variance of “genomic vectors” (i.e., linear combinations of SNP genotypes) using a Monte Carlo method. The method proceeds as follows:

1. Sample a vector of weights (b_s) completely at random (e.g., from a standard Gaussian distribution).
2. Compute the underlying genomic value by forming the linear combination: $g_s = Xb_s$.
3. Estimate the proportion of variance of g_s that can be explained by regression on haplotype blocks.
4. Repeat 1–3 for a large number of random vectors b_s .

In contrast to commonly used methods, like canonical correlation (Witten *et al.* 2009), this method is asymmetric in that it leads to different results by switching the roles of X and Z . The underlying genomic value is then generated based on the block dataset ($g_s = Zb_s$), and regressed on the SNP dataset X . Since we compute the share of the variance of one dataset explained by the other dataset, the share of variation that is not explained can be interpreted as previously underused information. An example of underused information is the local epistatic interactions that can be modeled via a block but are usually not fully captured by linear regression on single markers.

Recent work by Schreck and Schlather (2018) has suggested that the direct estimation of the heritability using REML variance components is biased, so we use their proposed estimator. For the traditional estimates using REML estimates as proposed in a conference presentation by de los Campos (2017), we refer to Table S1. Overall, the results were similar.

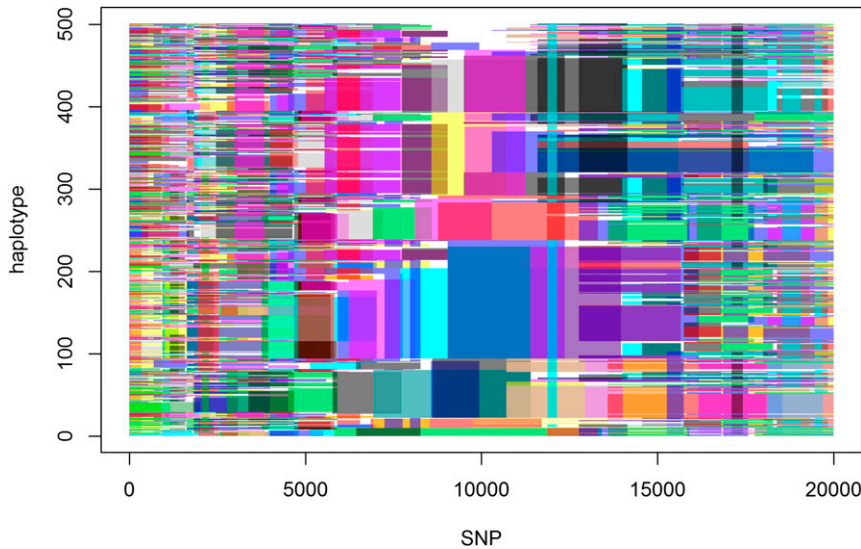


Figure 5 Graphical representation of the block structure for the first 20,000 SNPs of chromosome 1 in the KE DH lines. Haplotypes are sorted for similarity in SNP 10,000. In that region block structures are most visible, and transitions between blocks can be tracked easily. Further away from the center the representation gets fuzzy.

Recovering founder haplotypes

HaploBlocker does not require, or make use of, pedigree or founder haplotypes, but rather provides a method to recover haplotypes from the founders (or a genetic bottleneck) based solely on a genetic dataset of the current generation. To evaluate the ability to recover founder haplotypes, we simulated the generation of a multiparent advanced generation intercross population (MAGIC) based on the breeding scheme given in Zheng *et al.* (2015). Simulations were performed with the R-package MoBPS (R Core Team 2017; Pook 2019) with 19 founding haplotypes, intercrossing with a diallel design, four generations of random mating, and 10 generations of self-fertilization (Zheng *et al.* 2015). Each generation contains $\frac{19 \cdot 18}{2} = 171$ offspring. Genotypes of founders were assumed to be fully homozygous, with uniformly distributed minor allele frequencies, and under the assumption of equidistant markers (50k markers, one chromosome with a length of 3 Morgan, mutation rate of 10^{-4} in each marker). The haplotype phase of the final generation of offspring was assumed to be known. For the programming code used to perform the simulation in MoBPS (R Core Team 2017; Pook 2019), we refer to File S4.

Block-based EHH and IHH

Since haplotype blocks and SNPs are structurally different, blocks cannot be used directly in some methods developed for SNPs. The following shows how to adapt the EHH statistic (Sabeti *et al.* 2002, 2007) to be calculated based on haplotype blocks. EHH based on SNPs is defined as the probability of a segment between two markers to be in IBD, and can be estimated as:

$$EHH = \frac{\sum_i \binom{n_i}{2}}{\binom{N}{2}}.$$

Here, N is the total number of haplotypes and n_i is the number of occurrences of a given allelic sequence between the markers. In a second step, IHH (Voight *et al.* 2006) for a single marker is defined as the integral when calculating EHH of that marker to adjacent markers (until EHH reaches 0.05).

This concept can be extended to an EHH that is based on haplotype blocks (bEHH). Instead of calculating EHH for each marker, segments between the block boundaries (a_1, a_2, a_3, \dots) of haplotype blocks are considered jointly. Here, a_i is a physical position (e.g., in base pairs) in the genome. The set of block boundaries contains all start points of blocks, as well as all markers directly after a block (but not the end point itself). bEHH between segments $[a_i, a_{i+1} - 1]$ and $[a_j, a_{j+1} - 1]$ is then defined as the probability of two randomly sampled haplotypes belonging to the same haplotype block, or at least to a block with the same allelic sequence in the window $[a_i, a_{j+1} - 1]$ (with $i \leq j$). bEHH between two markers is set equal to bEHH between the two respective segments. IHH and derived test statistics like XP-EHH or iHs (Sabeti *et al.* 2007) can then be defined along the same lines as with single marker EHH. For a toy example on the computations necessary to compute EHH and bEHH, we refer to Figure S1 and File S3.

Overall, bEHH can be seen as an approximation of EHH. Computing times are massively reduced, since bEHH scores only need to be computed between pairs of segments instead of SNPs, overall leading to $\frac{p \cdot (p+1)}{2}$ necessary computations, with p being the number of segments and SNPs, respectively. Second, only allelic sequences of different haplotype blocks, instead of individual haplotypes between the two segments need to be compared for each calculation of bEHH.

As minor deviations from the joint allelic sequence of a haplotype block are possible, the usage of bEHH also provides robustness against calling errors and minor deviations.

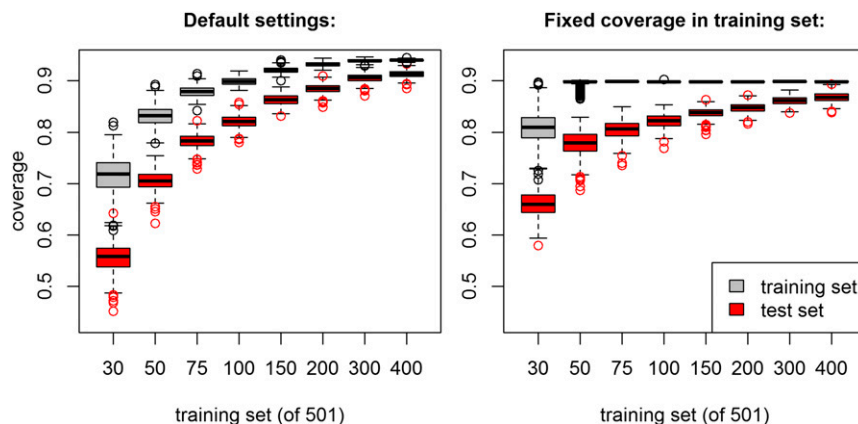


Figure 6 Proportion of the dataset represented by the haplotype library (coverage) of the training and test set in regard to size of the training set for chromosome 1 in the KE DH lines.

Genotype data used

We applied HaploBlocker to multiple datasets from different crop, livestock, and human populations. In the following, we report results obtained with a dataset of doubled haploid (DH) lines of two European maize (*Zea mays*) landraces [$n = 501$ Kemater Landmais Gelb (KE) and $n = 409$ Petkuser Ferdinand Rot (PE)] genotyped with the 600k Affymetrix Axiom Maize Genotyping Array (Unterseer *et al.* 2014) containing 616,201 markers (609,442 SNPs and 6759 short indels). Markers were filtered for assignment to the best quality class (PolyHighResolution; Pirani *et al.* 2013) and having a callrate of $\geq 90\%$. Since we do not expect heterozygous genotypes for DH lines, markers showing an excess of heterozygosity might result from unspecific binding at multiple sites of the genome. Thus, markers were also filtered for having $< 5\%$ heterozygous calls. This resulted in a dataset of 501,124 usable markers. The remaining heterozygous calls of the dataset were set to NA, and imputed using BEAGLE 4.0 (Browning and Browning 2016) with modified imputing parameters (buildwindow = 50, nsamples = 50, phase-its = 15).

Second, we used a dataset containing $n = 48$ S_0 plants from KE being generated from the same seed batch as the DH lines. Since S_0 are heterozygous, this corresponds to $n = 96$ haplotypes. Genotyping and quality control was performed in the same way as for the DH lines, without heterozygosity filters. After imputation, an additional phasing step for the S_0 using BEAGLE 4.1 (iterations = 15) was performed. In both steps, the DH lines were used as a reference panel. Only markers overlapping with the DH dataset were included. This resulted in a second dataset containing $n = 96$ S_0 and $n = 501$ DH haplotypes of KE and 487,462 markers.

Additionally, we used datasets from the 1000 Genomes Project phase 3 reference panel (1000 Genomes Project Consortium 2015) containing 5008 haplotypes, with a total of 88.3 million markers.

Data availability

The genetic data for maize, the associated R-package, the source code, and a detailed documentation of the package is available at <https://github.com/tpook92/HaploBlocker>. Genetic data from

the 1000 Genomes Project (1000 Genomes Project Consortium 2015) is available at <ftp://ftp.1000genomes.ebi.ac.uk/vol1/ftp/release/20130502/>.

File S1 provides an additional method section on the fitting procedure to obtain a certain target coverage. File S2 contains an additional method section on how to sort haplotypes for the graphical representation of haplotype blocks. File S3 provides an additional method section in which a toy example for the calculation of beHH is discussed. File S4 includes the R-code used to generate an exemplary MAGIC population for the section on recovering founder haplotypes. Table S1 contains the proportion of variance explained between the full SNP dataset, a SNP subset, and the block dataset using traditional heritability estimation as in de los Campos (2017). Table S2, Table S3, and Table S4 contain results obtained in Table 3, Table 4, and Table 5 when additionally using a target coverage of 95%. Figure S1 contains the dataset used in File S3. Figure S2 gives a comparison of the block structure in HaploBlocker and a bifurcation plot (Sabeti *et al.* 2002; Gautier and Vitalis 2012). Finally, Figure S3 provides a comparison of the block structure for different parameter settings of MCMB. Supplemental material available at FigShare: <https://doi.org/10.25386/genetics.7862525>.

Results and Discussion

Here, we will focus on the results obtained for chromosome 1 (80,200 SNPs) of the landrace KE. All evaluations were also performed for all other chromosomes and the second landrace (PE) with similar results.

Using the previously described default settings of HaploBlocker, we identified 477 blocks, which represent a coverage of 94.4% of the dataset and have an average length of 2575 SNPs (median: 1632 SNPs). For the whole genome, we identified 2991 blocks, representing 94.1% of the dataset with an average/median length of 2685/1301 SNPs. A graphical representation of the block structure for the first 20,000 markers of the set is given in Figure 5. Haplotypes were sorted according to their similarity at SNP 10,000. Since there is only limited linkage between markers that are further apart,

Table 6 Proportion of variance explained between the full SNP dataset (X), a SNP subset (X_s) and the block dataset (Z)

Number of Blocks/SNPs	$X \sim Z$ (%)	$Z \sim X$ (%)	$X \sim X_s$ (%)
1720	99.6	97.8	99.2
878	98.6	96.9	98.0
621	97.5	95.8	96.8
477	96.2	95.3	95.4
362	94.8	94.5	93.5
274	92.8	93.8	91.0
150	86.7	92.0	82.7

For comparability the number of parameters in X_s and Z were chosen equally.

the graphical representation becomes increasingly fuzzy with increasing distance from the target SNP. For a comparison to a bifurcation plot (Sabeti *et al.* 2002; Gautier and Vitalis 2012) of that marker, we refer to Figure S2.

When further investigating cells of the SNP dataset that are not covered by any of the haplotype blocks, one can typically observe that, in the associated segments, the allelic sequence of the haplotype is a combination of multiple identified haplotype blocks, and, by this, indicating a recent recombination. Start and end points of blocks can be seen as candidates for positions of ancient (or at least nonrecent) recombination, especially when multiple blocks start and end in the same region (e.g., between markers 8572 and 8601 in Figure 5).

In the following, we will show and discuss the influence of certain parameter settings on the resulting haplotype library. Results will be evaluated according to the number of blocks, their length, and the coverage of the haplotype library. Note that, even though differences seem quite substantial, most haplotype libraries actually contain the same core set of haplotype blocks, which are the most relevant under basically any parameter setting. Parameter settings mostly influence which of the less relevant blocks are included. By this, one can explicitly include a higher share of longer blocks, and obtain a certain coverage or similar. For most routine applications, the use of the default settings with a target coverage should be sufficient.

Effect of change in the MCMB

The MCMB affects both the number of blocks and the coverage of the dataset (Table 2). Higher MCMB leads to a stronger filtering of the haplotype blocks, and, thus, to a haplotype library with lower coverage and decreased number of larger blocks. Overall, MCMB is the most important parameter to balance between conservation of information (coverage) and dimension reduction (number of blocks). It should be noted that the ideal parametrization of MCMB depends highly on data structure (e.g., marker density). Instead of using a set value for MCMB, we recommend to fit the parameter automatically by setting a target coverage. For a graphical comparison of the structure of haplotype libraries with MCMB equal to 1000, 5000, and 20,000, we refer to Figure S3.

Table 7 Estimated genomic values using an OLS model assuming additive effects of single markers

Allelic sequence	Genomic value	Estimated genomic value
111	1	0.75
100	0	-0.25
011	0	0
110	0	0.25
101	0	0.25

Controlling length and number of haplotypes per block

The window size chosen in the cluster-building step has a notable influence on the window cluster. By using a smaller window size in the cluster-building step, the resulting groups are bigger, leading to more and shorter (in terms of physical length) haplotype blocks in the block-identification step (Table 3). As haplotype blocks are much larger than the window size in this case, the effects on the resulting haplotype library are only minor.

In the block-filtering step, the weighting between segment length (w_l) and number of haplotypes (w_n) in each block influences the structure of the later obtained haplotype library (Table 4). As one would expect, a higher weighting for the length of a block leads to longer blocks that include fewer haplotypes. The effect of a lower relative weighting for the number of haplotypes in each block was found to have only a minor effect in our maize data. A possible reason for this is that, even when using $w_l = w_n$, the longest blocks previously identified were already selected in the haplotype library.

When using the extended-block-identification method, the average length of finally obtained haplotype blocks is massively increased in the obtained haplotype library (Table 5). Additionally, overlap between blocks is increased. Using this procedure will lead to the identification of the longest possible IBD segments, making it especially useful for applications like BEHH and IHH.

Evaluations in this subsection were also performed when using a target coverage of 95%. For results here, we refer to Table S2, Table S3, and Table S4). Overall, results are similar.

Haplotypes from the sample

To assess how well HaploBlocker identifies haplotype block structures that also pertain to haplotype structures of other datasets, we split the maize data into a training and testing set, and compared the share of both datasets represented by a haplotype library based on the training set alone. In all cases, the coverage in the test set was below that of the training set, but with higher numbers of haplotypes in the training set the differences gets smaller. In the case of 400 haplotypes in the training set and 101 haplotypes in the test set, the difference in coverage is as low as 2.7% (Figure 6), indicating

Table 8 Structure of the haplotype library under different marker densities using the adaptive mode in HaploBlocker with target coverage of 95% for chromosome 1 in the KE DH lines

Density	Number of Blocks	Average block length (# of SNPs on full array)	Haplotypes per Block	Used MCMB
Every SNP	534	2317	116.4	2813
Every second SNP	523	2281	112.7	1563
Every fifth SNP	450	2557	96.9	945
Every tenth SNP	401	2811	90.6	758
Every fortieth SNP	319	3637	79.9	294

that haplotype libraries derived in a sufficiently large dataset can be extended to individuals outside of the sample if they have similar genetic origin. Similar results were obtained when setting a target coverage (90%) for the test set.

Information content

We investigated the information content between the SNP and block dataset according to the method described above (de los Campos 2017), where b_s was sampled from a standard Gaussian distribution. A REML approach was used for fitting the model. We found that, on average, 96.0% of the variance of the SNP dataset can be explained by the default haplotype library (Table 6). As one would expect, the share of variance explained is increasing when increasing the number of blocks in the haplotype library. On the other hand, the share of the variance of the haplotype library that can be explained by the SNP dataset is 95.2%. Even though the number of parameters in the block dataset (Z) is much smaller than in the full SNP set (X), the share of the variance explained by the corresponding dataset is similar.

When using a subset of markers (X_s) with the same number of SNPs as haplotype blocks in the haplotype library, the share of variation explained is slightly lower (95.1%) than for the block dataset. Unlike the haplotype library, the variation in the SNP subset is basically fully explained by the full SNP dataset ($\geq 99.99\%$). This should not be surprising, since X_s is a genuine subset of X . Even though a similar share in variation of the SNP dataset is preserved, the block dataset should be preferred as it is able to incorporate effects that are not explained by linear effects of single markers.

With the following toy example, we illustrate what kind of effects can be grasped by a block dataset compared to a model that is only assigning effects to single markers, as is done in GBLUP (Meuwissen *et al.* 2001) using the traditional genomic relationship matrix (VanRaden 2008). Consider a dataset (Table 7) with three markers, five haplotypes and a genomic value of 1 for the allelic sequence 111. When assuming no environmental effects, phenotypes equal to genomic values and fitting an ordinary least squares model (OLS) on single markers, the resulting model estimates effects of 0.75, 0.5,

Table 9 Structure of the haplotype library under different marker densities when adjusting parameters according to data structure for chromosome 1 in the KE DH lines

Density	Number of Blocks	Average block length (# of SNPs on full array)	Haplotypes per Block	Coverage (%)
Every SNP	474	2615	101.4	95.0
Every 2nd SNP	474	2720	108.1	95.1
Every 5th SNP	481	2557	115.4	95.1
Every 10th SNP	520	2174	142.7	95.8
Every 40th SNP (MCMB = 125)	522	2056	172.9	97.9
Every 40th SNP (MCMB = 250)	404	2287	166.0	96.6

and 0.5 for the three respective alleles with an intercept of -1 . Overall, single marker effects can approximate, but not fully explain, an underlying epistatic genomic value (Table 7), whereas a block dataset allows for a natural model of effects caused by local interactions.

Overlapping segments in multiple landraces

When using HaploBlocker on the joint dataset of both landraces (KE and PE), the resulting haplotype library contains essentially the same haplotype blocks that were identified in the haplotype libraries derived for the two landraces individually. The reason for this is that segments shared between landraces are often short, leading to a small rating r_b , and, thus, removal in the block-filtering step. To specifically identify those sequences that are present in both landraces, we added the constraint that each block had to be present in at least five haplotypes of both landraces. This results in the identification of 1655 blocks that are present in both landraces. Those blocks are much shorter (average length: 207 SNPs) and represent only 62.7% of the genetic diversity of the dataset. This is not too surprising since the haplotypes of a single landrace are expected to be much more similar than haplotypes from different landraces. Explicitly, this is not an indicator for 62.7% of the chromosome of both landraces to be the same. Shared haplotype blocks can be found across the whole chromosome, but only some haplotypes of the landraces have those shared segments.

Comparison with the results of HaploView

Overall, the structure of the haplotype blocks generated with our approach is vastly different from blocks obtained with LD-based approaches such as HaploView (Barrett *et al.* 2005). When applying HaploView on default settings (Gabriel *et al.* 2002) to chromosome 1 of the maize data, 2666 blocks are identified (average length: 27.8 SNPs, median: 20 SNPs), and 4865 SNPs (6.1%) are not contained in any block. If one were to use a similar coding for the blocks obtained in HaploBlocker, and use a separate variable for each allelic sequence in a block, one would have to account for 12,550



Figure 7 Estimated and true founders for five representative haplotypes of the last generation of a MAGIC population simulated according to breeding scheme given in Zheng *et al.* (2015) using a target coverage of 95% in the generation of the haplotype library. Segments are colored according to the originating/estimated haplotype of the founder generation.

different allelic sequences (excluding singletons). For the whole genome, this would result in 16,904 blocks with 79,718 allelic sequences. When using a dataset with both landraces (or, in general, more diversity), LD-based blocks get even smaller (for chromosome 1: 4367 blocks, 24,511 different allelic sequences, average length: 17.3 SNPs, median: 9 SNPs, 4718 SNPs in no block). In comparison, the haplotype library identified in HaploBlocker with multiple landraces is, with minor exceptions, a combination of the two single landrace haplotype libraries (1112 blocks, average length: 2294 SNPs, median: 1402 SNPs, coverage: 94.4%). Overall, the potential to detect long range associations between markers and to reduce the number of parameters in the dataset is much higher when using haplotype blocks generated by HaploBlocker.

Differences between the two methods become even more drastic when applying HaploView to the human datasets generated in the 1000 Genomes Project Phase 3 (1000 Genomes Project Consortium 2015). For chromosome 22, there were 49,504 blocks, with an average length of 199 SNPs (median: 81 SNPs) that cover 92.9% of the dataset in HaploBlocker. In contrast, there were only 12,304 blocks (excluding singletons) identified in HaploView (average length: 8.1 SNPs, median: 4 SNPs), but only 99,130 of the 424,147 markers were assigned to a block (23.4%). In total, there were still 544,038 different allelic sequences in the identified blocks in HaploView. We noted that all alternative variants were coded as the same allele, as HaploView is able to handle only two alleles per marker, while HaploBlocker is able to handle up to 255 different alleles per marker. When allowing for more than two alleles per marker in HaploBlocker, we obtain 49,500 blocks with an average length of 200 SNPs (median: 81 SNPs) that cover 93.0% of the dataset. It should be noted that HaploView was developed with different objectives in mind (Barrett *et al.* 2005).

Influence of marker density

A common feature of conventional approaches to identify haplotype blocks is that, with increasing marker density, the physical size of blocks is strongly decreasing (Sun *et al.* 2004; Kim and Yoo 2016). To assess this, we executed HaploBlocker on datasets with different marker densities by including only every second/fifth/tenth/fortieth marker of the maize dataset in the model. Since the physical size of a window

with a fixed number of markers is vastly different, we compared the structure of the obtained haplotype library using the adaptive mode in HaploBlocker (multiple window clusters with window sizes 5,10,20,50 and adaptive MCMB to obtain a target coverage of 95%) instead of default settings. As there are far fewer markers with possible variation, fewer blocks are needed to obtain the same coverage in the low-density datasets (Table 8). Since windows in the cluster-building-step span over a longer part of the genome, the considered groups contain fewer haplotypes, leading to less frequent nodes in the window cluster. Since the haplotypes in a node are, on average, more related to each other, the identified blocks tend to be longer and include fewer haplotypes.

In a second step, we manually adapted the window size (50/25/10/5/5) and the MCMB (5000/2500/1000/500/125) according to the marker density of the dataset. When manually adapting the parameters, the number of blocks in the haplotype library is largely independent of the marker density (Table 9). The length of the blocks is decreasing, whereas the number of haplotypes per block is increasing with decreasing marker density. A possible reason for this is that haplotypes in the same node of the window cluster are less similar in the region than when using bigger window sizes. This will lead to shorter haplotype blocks that are carried by more but less related haplotypes. In the case of the dataset in which we used every 40th marker, we additionally considered a value of 250 for the MCMB, since the resulting coverage was a lot higher, indicating that less overall variation is present in the dataset. This also results in fewer overall blocks needed to obtain similar coverage.

Haplotype libraries for all considered marker densities were similar, indicating that, for our landrace population, a much lower marker density would have been sufficient to derive haplotype blocks via HaploBlocker. If the physical size of haplotype blocks is smaller, a higher marker density is needed.

Recovering founder haplotypes

HaploBlocker was applied to the final generation of the dataset simulated in analogy to the breeding scheme for the MAGIC population given in Zheng *et al.* (2015). On average, we obtained 827 haplotype blocks with a length of 1420 markers covering 82.8% of the dataset; 96.0% of the allelic sequences of haplotype blocks are $\geq 99\%$ the same as

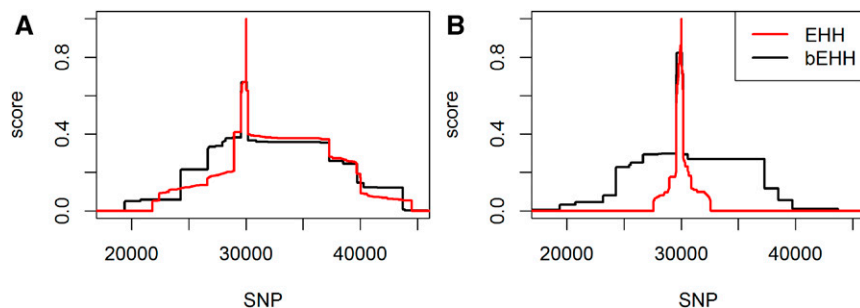


Figure 8 Comparison of EHH and bEHH scores for DH lines (A) and S_0 (B) for marker 30,000 of chromosome 1 in the KE DH-lines.

an allelic sequence of a founder haplotype of that segment. Overall, 86.6% of all cells in the SNP dataset of the founders are recovered by the resulting haplotype library. When using a target coverage of 95%, the share of the allelic sequences of the blocks that are the same as a founder haplotype is quite similar (96.6%), but 93.6% of all cells of the SNP dataset of the founders can be recovered. Note that identified haplotype blocks, by default, have a minimum size of five haplotypes, leading to the loss of rarely inherited haplotypes.

It should be noted that our approach is not constructed to detect the exact boundaries of IBD segments between founders and single offspring, but, instead, it detects commonly presented allelic sequences. In a population with limited founders (e.g., caused by a genetic bottleneck), those common allelic sequences most likely stem from the founders of the population. For a plot comparing the true and estimated genetic origin of the final generation, we refer to Figure 7. Here, estimation means that, if a haplotype block completely stems from a single founder, that particular founder is used as the origin. Note that haplotype blocks are much shorter than the size of segments originating from a particular founder, leading to multiple haplotype blocks that all correspond to a part of a segment inherited from a particular founder, and, therefore, are colored the same in Figure 7. For details on the whole selection procedure, we refer to File S4. In practice, nonoverlapping blocks cannot, of course, be assigned to the same founder. The main benefit of our method is that, in contrast to commonly used methods, only phased genotype data are needed to recover founder haplotypes. When

interest is in the exact boundaries of IBD segments for single haplotypes and founders (with known pedigree), we recommend the use of methods like RABBIT (Zheng *et al.* 2015).

Block-based selection signatures

When deriving EHH and bEHH scores, we observed that the curves were quite similar for DH lines (Figure 8). The most apparent difference was a much higher EHH score in the region directly surrounding the marker. Those segments are typically much smaller than the segments considered jointly in the bEHH approach. Note that the same allelic sequence in such a small region can occur not only based on IBD but also by chance. On the contrary, scores between distant markers for the S_0 plants were much lower when using EHH (Figure 8). This is caused mainly by the incorporated robustness of bEHH, since the S_0 dataset tends to contain a higher share of minor deviations between haplotypes.

When using EHH (Sabeti *et al.* 2002) to derive IHH (Voight *et al.* 2006), the selection pressure on DH-lines is estimated to be much higher, whereas scores are quite similar between the two groups when using bEHH (Figure 9). IHH scores based on bEHH are in concordance with previous research, as we would expect little to no loss of diversity or selection in the process of generating DH-lines (Melchinger *et al.* 2017). Results in Melchinger *et al.* (2017) were derived by the use of F_{st} (Holsinger and Weir 2009) and analysis of molecular diversity in single markers. As presented at a recent conference (Mayer *et al.* 2018), similar studies with matching results were also performed for KE and PE.

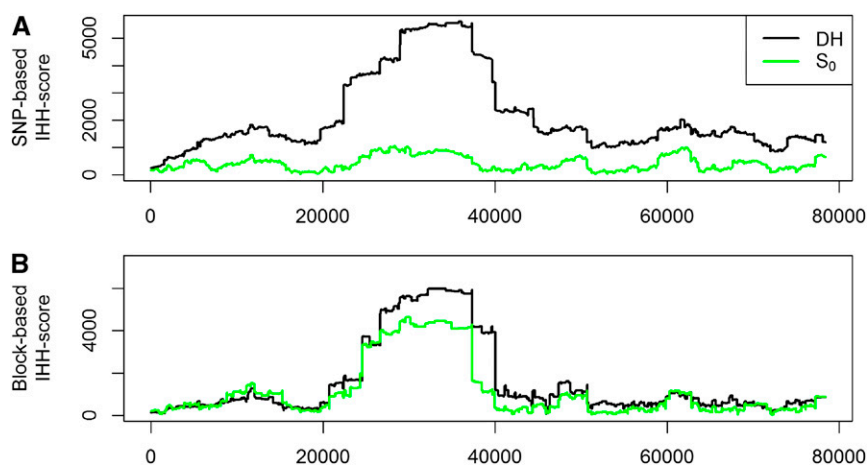


Figure 9 IHH scores based on SNPs (A) and haplotype blocks (B) for DH lines and S_0 for chromosome 1 in the KE.

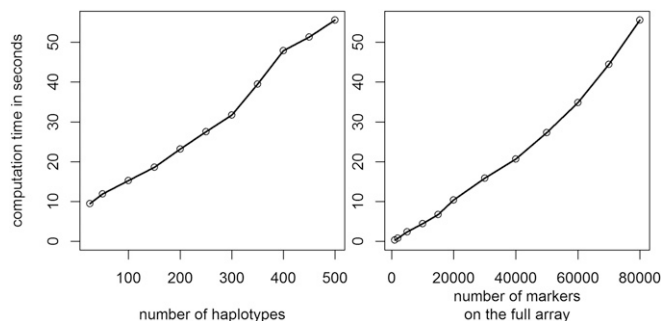


Figure 10 Comparison of computing times for datasets of various sizes for chromosome 1 in the KE DH lines.

Computing time

Overall computing times were not an issue for the considered datasets when using the associated R-package HaploBlocker (R Core Team 2017; Pook and Schlather 2019) with the full dataset (501 haplotypes, 80,200 SNPs) needing 55 sec on default, 75 sec with a target coverage and 13.3 min in adaptive mode. Computations were performed on a single core of a server cluster with Broadwell Intel E5-2650 (2×12 core 2.2 GHz) processors. Most crucial parts in terms of computing time are written in C.

For our datasets, computing time scaled approximately linearly in both number of haplotypes and the physical size of the genome analyzed (Figure 10). Especially for the number of haplotypes, it is difficult to generalize because the number of nodes in the window cluster is the main cause of the increase in computing time. The marker density had only a minor effect. Even a panel containing just every tenth marker, on average, needed 99.3% of the computing time of the full dataset.

Conclusions and outlook

HaploBlocker provides a natural technique to model local epistasis, and thereby solves some of the general problems of markers being correlated but not causal individually (Akdemir *et al.* 2017; He *et al.* 2017). This can be seen as one of the factors contributing to the “missing heritability” phenomenon in genetic datasets (Manolio *et al.* 2009). The haplotype blocks obtained are a concise representation of the variation present in a SNP dataset. The block assignment in HaploBlocker is deterministic and does not incorporate uncertainty, although the algorithm provides flexibility to control the structure of the haplotype library via parameter tuning.

Even though results were presented mainly for a maize dataset containing DH lines, methods are not species-dependent or limited to fully homozygous individuals. Methods were also applied to livestock and human data. As HaploBlocker is not able to handle uncertainty in haplotype phase assignment, an initial phasing step is mandatory. For human data, in particular, this can be a substantial application problem,

requiring triplet data or high-quality phase such as that available in the 1000 Genomes Project (1000 Genomes Project Consortium 2015). Overall, the opportunities for identifying long, shared segments will be higher in SNP datasets from populations subjected to a recent history of intensive selection, as is commonly present in livestock and crop datasets. Recent work has suggested that the phasing accuracy for these kinds of datasets is extremely high (Pook *et al.* 2019) and should, therefore, be sufficient for the application of HaploBlocker. For datasets containing less related individuals, as commonly present in human data, poor phasing accuracy can limit the applicability and usefulness of HaploBlocker.

It should be noted that, by using blocks, no assignment of effects to physical positions (like in a typical GWAS study) is obtained. A subsequent analysis is needed to identify which segment of the significantly trait-associated haplotype block is causal for a trait, and/or which parts of that block differ from other blocks in that region.

A future topic of research is the explicit inclusion of larger structural variation like duplications, insertions, or deletions as is done in methods to generate a pangenome (Eggertsson *et al.* 2017). Since blocks in HaploBlocker are of large physical size, most structural variation should still be modeled implicitly, and application to sequence data is perfectly possible.

HaploBlocker provides an innovative and flexible approach to screen a dataset for block structure. The representation and condensation of a SNP dataset as a block dataset enables new methods for further genomic analyses. For some applications, already existing techniques for a SNP dataset can be applied directly by using a block dataset instead (e.g., genomic prediction). For other applications, like the detection of selection signatures via EHH/IHH, modifications of the original methodology are needed. Features of HaploBlocker can even enhance existing methods and lead to improvements such as an increased robustness of the methods against minor variation, or a massively reduced computing time. Additionally, problems regarding typical $p \gg n$ -settings in genetic datasets (Fan *et al.* 2014) can be heavily reduced, allowing for the usage of more complex statistical models that include epistasis or even apply deep learning methods with a reduced risk of over-fitting.

Acknowledgments

We thank Nicholas Schreck for useful comments on the manuscript and his help regarding unbiased heritability estimation. The authors further thank the German Federal Ministry of Education and Research (BMBF) for the funding of our project (MAZE – “Accessing the genomic and functional diversity of maize to improve quantitative traits”; Funding ID: 031B0195). G.d.l.C. was supported by a Mercator-fellowship of the German Research Foundation (DFG) within the Research Training Group 1644, “Scaling problems in statistics” (grant no. 152112243).

Literature Cited

- 1000 Genomes Project Consortium, Auton, A., L. D. Brooks, R. M. Durbin, E. P. Garrison, and H. M. Kang *et al.*, 2015 A global reference for human genetic variation. *Nature* 526: 68–74. <https://doi.org/10.1038/nature15393>
- Akdemir, D., J.-L. Jannink, and J. Isidro-Sánchez, 2017 Locally epistatic models for genome-wide prediction and association by importance sampling. *Genet. Sel. Evol.* 49: 74. <https://doi.org/10.1186/s12711-017-0348-8>
- Barrett, J. C., B. Fry, J. Maller, and M. J. Daly, 2005 Haploview: analysis and visualization of ld and haplotype maps. *Bioinformatics* 21: 263–265. <https://doi.org/10.1093/bioinformatics/bth457>
- Browning, B. L., and S. R. Browning, 2007 Efficient multilocus association testing for whole genome association studies using localized haplotype clustering. *Genet. Epidemiol.* 31: 365–375. <https://doi.org/10.1002/gepi.20216>
- Browning, B. L., and S. R. Browning, 2013 Improving the accuracy and efficiency of identity-by-descent detection in population data. *Genetics* 194: 459–471. <https://doi.org/10.1534/genetics.113.150029>
- Browning, B. L., and S. R. Browning, 2016 Genotype imputation with millions of reference samples. *Am. J. Hum. Genet.* 98: 116–126. <https://doi.org/10.1016/j.ajhg.2015.11.020>
- Covarrubias-Pazaran, G., 2016 Genome-assisted prediction of quantitative traits using the r package sommer. *PLoS One* 11: e0156744. <https://doi.org/10.1371/journal.pone.0156744>
- Daly, M. J., J. D. Rioux, S. F. Schaffner, T. J. Hudson, and E. S. Lander, 2001 High-resolution haplotype structure in the human genome. *Nat. Genet.* 29: 229–232. <https://doi.org/10.1038/ng1001-229>
- Danecek, P., A. Auton, G. Abecasis, C. A. Albers, E. Banks *et al.*, 2011 The variant call format and vcftools. *Bioinformatics* 27: 2156–2158. <https://doi.org/10.1093/bioinformatics/btr330>
- de los Campos, G., 2017 What fraction of the information contained in an omic set can be explained by other omics? paper # 22987. Plant and Animal Genome Conference, San Diego, California.
- Druet, T., and M. Georges, 2010 A hidden Markov model combining linkage and linkage disequilibrium information for haplotype reconstruction and quantitative trait locus fine mapping. *Genetics* 184: 789–798. <https://doi.org/10.1534/genetics.109.108431>
- Eggertsson, H. P., H. Jonsson, S. Kristmundsdottir, E. Hjartarson, B. Kehr *et al.*, 2017 GraphTyper enables population-scale genotyping using pangenome graphs. *Nat. Genet.* 49: 1654–1660. <https://doi.org/10.1038/ng.3964>
- Fan, J., F. Han, and H. Liu, 2014 Challenges of big data analysis. *Natl. Sci. Rev.* 1: 293–314. <https://doi.org/10.1093/nsr/nwt032>
- Gabriel, S. B., S. F. Schaffner, H. Nguyen, J. M. Moore, J. Roy *et al.*, 2002 The structure of haplotype blocks in the human genome. *Science* 296: 2225–2229. <https://doi.org/10.1126/science.1069424>
- Gautier, M., and R. Vitalis, 2012 Rehh: an r package to detect footprints of selection in genome-wide SNP data from haplotype structure. *Bioinformatics* 28: 1176–1177. <https://doi.org/10.1093/bioinformatics/bts115>
- He, D., 2013 IBD-groupon: an efficient method for detecting group-wise identity-by-descent regions simultaneously in multiple individuals based on pairwise IBD relationships. *Bioinformatics* 29: i162–i170. <https://doi.org/10.1093/bioinformatics/btt237>
- He, S., J. C. Reif, V. Korzun, R. Bothe, E. Ebmeyer *et al.*, 2017 Genome-wide mapping and prediction suggests presence of local epistasis in a vast elite winter wheat populations adapted to central Europe. *Theor. Appl. Genet.* 130: 635–647. <https://doi.org/10.1007/s00122-016-2840-x>
- Holsinger, K. E., and B. S. Weir, 2009 Genetics in geographically structured populations: defining, estimating and interpreting f(st). *Nat. Rev. Genet.* 10: 639–650. <https://doi.org/10.1038/nrg2611>
- Islam, M. S., G. N. Thyssen, J. N. Jenkins, L. Zeng, C. D. Delhom *et al.*, 2016 A magic population-based genome-wide association study reveals functional association of ghrbb1_a07 gene with superior fiber quality in cotton. *BMC Genomics* 17: 903. <https://doi.org/10.1186/s12864-016-3249-2>
- Jiang, Y., R. H. Schmidt, and J. C. Reif, 2018 Haplotype-based genome-wide prediction models exploit local epistatic interactions among markers. *G3 (Bethesda)* 8: 1687–1699. <https://doi.org/10.1534/g3.117.300548>
- Kim, S. A., and Y. J. Yoo, 2016 Effects of single nucleotide polymorphism marker density on haplotype block partition. *Genomics Inform.* 14: 196–204. <https://doi.org/10.5808/GI.2016.14.4.196>
- Kim, S. A., C.-S. Cho, S.-R. Kim, S. B. Bull, and Y. J. Yoo, 2017 A new haplotype block detection method for dense genome sequencing data based on interval graph modeling of clusters of highly correlated SNPs. *Bioinformatics* 34: 388–397. <https://doi.org/10.1093/bioinformatics/btx609>
- Manolio, T. A., F. S. Collins, N. J. Cox, D. B. Goldstein, L. A. Hindorf *et al.*, 2009 Finding the missing heritability of complex diseases. *Nature* 461: 747–753. <https://doi.org/10.1038/nature08494>
- Mayer, M., T. Presterl, M. Ouzunova, E. Bauer, and C. C. Schoen, 2018 Representing allelic diversity of maize landraces by libraries of doubled-haploid lines: paper # 97. German Plant Breeding Conference, Wernigerode, Germany, pp. 138.
- Melchinger, A. E., P. Schopp, D. Müller, T. A. Schrag, E. Bauer *et al.*, 2017 Safeguarding our genetic resources with libraries of doubled-haploid lines. *Genetics* 206: 1611–1619. <https://doi.org/10.1534/genetics.115.186205>
- Meuwissen, T. H. E., B. J. Hayes, and M. E. Goddard, 2001 Prediction of total genetic value using genome-wide dense marker maps. *Genetics* 157: 1819–1829.
- Meuwissen, T. H. E., J. Odegard, I. Andersen-Ranberg, and E. Grindflek, 2014 On the distance of genetic relationships and the accuracy of genomic prediction in pig breeding. *Genet. Sel. Evol.* 46: 49. <https://doi.org/10.1186/1297-9686-46-49>
- Moltke, I., A. Albrechtsen, T. V. Hansen, F. C. Nielsen, and R. Nielsen, 2011 A method for detecting ibd regions simultaneously in multiple individuals—with applications to disease genetics. *Genome Res.* 21: 1168–1180. <https://doi.org/10.1101/gr.115360.110>
- Pattaro, C., I. Ruczinski, D. M. Fallin, and G. Parmigiani, 2008 Haplotype block partitioning as a tool for dimensionality reduction in snp association studies. *BMC Genomics* 9: 405. <https://doi.org/10.1186/1471-2164-9-405>
- Patterson, H. D., and R. Thompson, 1971 Recovery of inter-block information when block sizes are unequal. *Biometrika* 58: 545–554. <https://doi.org/10.1093/biomet/58.3.545>
- Pirani, A., H. Gao, L. Bellon, and T. A. Webster, 2013 2013 Best practices for genotyping analysis of plant and animal genomes with affymetrix axiom arrays. The International Plant and Animal Genome XXI Conference, Scherago International, San Diego, CA, pp. P0997.
- Pook, T., 2019 Mobps: modular breeding program simulator, r-package version 1.1.24. Available at: <https://github.com/tpook92/mobps>
- Pook, T., and M. Schlather, 2019 Haploblocker: creation of haplotype libraries for dhs and highly inbred lines, r-package version 1.4.7. Available at <https://github.com/tpook92/haploblocker>
- Pook, T., M. Mayer, J. Geibel, S. Weigend, D. Caverro *et al.*, 2019 Improving imputation quality in beagle for crop and livestock data. *bioRxiv*. <https://doi.org/10.1101/577338>

- Powell, M. J. D., 2009 The bobyqa algorithm for bound constrained optimization without derivatives. Cambridge NA Report NA2009/06. University of Cambridge, Cambridge, pp. 26–46.
- Purcell, S., B. Neale, K. Todd-Brown, L. Thomas, M. A. R. Ferreira *et al.*, 2007 Plink: a tool set for whole-genome association and population-based linkage analyses. *Am. J. Hum. Genet.* 81: 559–575. <https://doi.org/10.1086/519795>
- R Core Team, 2017 *R: A Language and Environment for Statistical Computing*. R Foundation for Statistical Computing, Vienna.
- Sabeti, P. C., D. E. Reich, J. M. Higgins, H. Z. P. Levine, D. J. Richter *et al.*, 2002 Detecting recent positive selection in the human genome from haplotype structure. *Nature* 419: 832–837. <https://doi.org/10.1038/nature01140>
- Sabeti, P. C., P. Varilly, B. Fry, J. Lohmueller, E. Hostetter *et al.*, 2007 Genome-wide detection and characterization of positive selection in human populations. *Nature* 449: 913–918. <https://doi.org/10.1038/nature06250>
- Schreck, N., and M. Schlather, 2018 From estimation to prediction of genomic variances: allowing for linkage disequilibrium and unbiasedness. *bioRxiv*. <https://doi.org/10.1101/282343>
- Slatkin, M., 2008 Linkage disequilibrium—understanding the evolutionary past and mapping the medical future. *Nat. Rev. Genet.* 9: 477–485. <https://doi.org/10.1038/nrg2361>
- Sun, X., J. C. Stephens, and H. Zhao, 2004 The impact of sample size and marker selection on the study of haplotype structures. *Hum. Genomics* 1: 179. <https://doi.org/10.1186/1479-7364-1-3-179>
- Taliun, D., J. Gamper, and C. Pattaro, 2014 Efficient haplotype block recognition of very long and dense genetic sequences. *BMC Bioinformatics* 15: 10. <https://doi.org/10.1186/1471-2105-15-10>
- Unterseer, S., E. Bauer, G. Haberer, M. Seidel, C. Knaak *et al.*, 2014 A powerful tool for genome analysis in maize: development and evaluation of the high density 600 k snp genotyping array. *BMC Genomics* 15: 823. <https://doi.org/10.1186/1471-2164-15-823>
- VanRaden, P. M., 2008 Efficient methods to compute genomic predictions. *J. Dairy Sci.* 91: 4414–4423. <https://doi.org/10.3168/jds.2007-0980>
- Voight, B. F., S. Kudaravalli, X. Wen, and J. K. Pritchard, 2006 A map of recent positive selection in the human genome. *PLoS Biol.* 4: e72 (erratum: *PLoS Biol.* 4: e154); [corrigenda: *PLoS Biol.* 5: e147 (2007)]. <https://doi.org/10.1371/journal.pbio.0040072>
- Wall, J. D., and J. K. Pritchard, 2003 Haplotype blocks and linkage disequilibrium in the human genome. *Nat. Rev. Genet.* 4: 587–597. <https://doi.org/10.1038/nrg1123>
- Witten, D. M., R. Tibshirani, and T. Hastie, 2009 A penalized matrix decomposition, with applications to sparse principal components and canonical correlation analysis. *Biostatistics* 10: 515–534. <https://doi.org/10.1093/biostatistics/kxp008>
- Zhang, K., P. Calabrese, M. Nordborg, and F. Sun, 2002 Haplotype block structure and its applications to association studies: power and study designs. *Am. J. Hum. Genet.* 71: 1386–1394. <https://doi.org/10.1086/344780>
- Zheng, C., M. P. Boer, and F. A. van Eeuwijk, 2015 Reconstruction of genome ancestry blocks in multiparental populations. *Genetics* 200: 1073–1087. <https://doi.org/10.1534/genetics.115.177873>

Communicating editor: W. Valdar